Published in final edited form as:
Nucl Med Biol. 2009 July ; 36(5): 489–493. doi:10.1016/j.nucmedbio.2009.02.007.

PET Imaging of (2*R*,3*R*)-5-[^{18}F]Fluoroethoxybenzovesamicol ((-)-FEOBV) in rat and monkey brain: A Radioligand for the Vesicular Acetylcholine Transporter

Michael R. Kilbourn, **Brian Hockley**, **Lihsueh Lee**, **Phillip Sherman**, **Carole Quesada**, **Kirk A. Frey**, and **Robert A. Koeppe**
Division of Nuclear Medicine, Department of Radiology, University of Michigan School of Medicine, Ann Arbor, MI 48109

Abstract

Introduction—The regional brain distribution of (2*R*,3*R*)-5-[[^{18}F]fluoroethoxy-benzovesamicol ((-)-[^{18}F]FEOBV), a radioligand for the vesicular acetylcholine transporter (VAChT), was examined in vivo in mice, rats, and rhesus monkeys.

Methods—Regional brain distributions of (-)-[^{18}F]FEOBV in mice were determined using ex vivo dissection. MicroPET imaging was used to determine the regional brain pharmacokinetics of the radioligand in rat and rhesus monkey brains.

Results—In all three species, clear heterogeneous regional brain distributions were obtained, with the rank order of brain tissues (striatum>thalamus>cortex>cerebellum) consistent with the distribution of cholinergic nerve terminals containing the VAChT.

Conclusions—(-)-[^{18}F]FEOBV remains a viable candidate for further development as an in vivo imaging agent for Positron Emission Tomography (PET) studies of the VAChT in the human brain.

Keywords

vesamicol; vesicular transporter; PET

1. Introduction

The vesicular acetylcholine transporter (VAChT) is a protein uniquely located in presynaptic vesicles of cholinergic neurons, and is responsible for the transport of the neurotransmitter acetylcholine into the storage vesicles [1]. As a specific biochemical function of the cholinergic neuron, it has been a potential target for development of in vivo radioligands [2,3] for SPECT (single photon emission computed tomography) or PET (positron emission tomography) imaging of the potential losses of cholinergic neurons in degenerative neurological diseases. Successful imaging of the VAChT in the human brain, including losses in disease including Alzheimer's, has been reported using a SPECT radioiodinated ligand 5-[^{123}I] iodobenzovesamicol ((-)-5-IBVM) [4,5,6,7]. For potential use in PET, radioligands labeled with the positron-emitting radionuclides carbon-11 and fluorine-18 were reported as early as

1990 [8,9] and there has been continued interest in further evaluation of both SPECTand PET radioligands for imaging of the VAChT binding site in the human brain [10,11].

Most recently, Giboureau and coworkers [10] reported the in vivo evaluation in rats and primate brain of two potential PET radioligands, (2*R*,3*R*)-5-[^{18}F]fluoroethoxybenzovesamicol ((-)-[^{18}F]FEOBV, first reported in 1993 by Mulholland et al [12]) and (2*R*,3*R*)-5-[^{18}F] fluoropropoxybenzovesamicol (((-)-[^{18}F]FPOBV). Using ex vivo dissection techniques for both radioligands, and in vivo PET imaging of [^{18}F]FPOBV in monkey brain, these investigators concluded that both (-)-[^{18}F]FEOBV and (-)-[^{18}F]FPOBV were unsuitable as in vivo radioligands for the imaging for the VAChT in the mammalian brain. Their report directly contradicts our earlier and extensive rodent studies of (-)-[^{18}F]FEOBV [13], which had consistently supported that it would be a viable candidate for further development as a PET imaging agent for human studies of the VAChT. As we have continued to pursue the development of (-)-[^{18}F]FEOBV with the intention of eventual human applications, we felt it was necessary to re-visit our in vivo studies of (-)-[^{18}F]FEOBV to verify our earlier conclusions. We report here in vivo studies of (-)-[^{18}F]FEOBV in mice, rats and non-human primates, including dynamic microPET imaging studies, which clearly demonstrate that (-)-[^{18}F]FEOBV is indeed a successful imaging agent for the VAChT and is worthy of further development and implementation.

2. Materials and Methods

2.1. Synthesis of (2R,3R)-5-[^{18}F]fluoroethoxybenzovesamicol ((-)-[^{18}F]FEOBV)

Syntheses of (-)-[^{18}F]FEOBV and unlabeled (-)-FEOBV were done by slight modifications of the literature procedure [12]. Reaction of the tosyloxy precursor, (2*R*,3*R*)-5-(2-tosyloxyethoxy) benzovesamicol , with no-carrier-added [^{18}F]fluoride ion in dimethylsulfoxide followed by purification using preparative high pressure liquid chromatography provided the desired (-)-[^{18}F]FEOBV is high radiochemical purity (>95%) and specific activities of 3500-13300 Ci/mmol at end of synthesis. For the monkey PET imaging studies the synthesis was fully automated using a General Electric Medical Systems TracerLab FX F N synthesis box.

2.2. Regional mouse brain biodistribution and blocking studies

Studies were done in young male CD-1 mice (20-25 g). Animals were anesthetized withdiethyl ether and injected via the tail vein with 7.7 – 24.5 microcuries (7-22 nanograms) of (-)-[^{18}F] FEOBV co-injected with saline (N = 18), or 2 (N = 6), 5 (N = 6) or 10 (N = 3) micrograms/kg of unlabeled (-)-FEOBV. Animals were then allowed to awaken. At 180 min, animals were killed and the brains removed and dissected into the following regions of interest: striatum, cortex, hippocampus, thalamus and cerebellum. Tissue samples were weighed and counted for radioactivity, and the percent injected dose per gram (%ID/g) calculated. Differences between (-)-FEOBV-treated groups and the control group were evaluated using a Student's t-test with $p < 0.05$ as significance level.

2.3. Rat microPET Imaging

Studies were done in young mature male CD-1 rats (260-265 g). Animals were anesthetized with isoflurane, a catheter inserted into the tail vein, and the animals positioned in the gantry of the microPET scanners (both concorde MicroPET R4 and P4 scanners used). After completion of the attenuation scan, animals were injected with a bolus of (-)-[^{18}F]FEOBV (1.38 and 1.44 mCi, 0.12 and 0.13 micrograms) and imaged for 70 minutes. Emission data were corrected for attenuation and scatter and reconstructed using the 3D maximum a priori method (3D MAP algorithm). Using a summed image of the last two frames (50-70 min), ROIs were drawn manually on multiple planes to obtain volumetric ROIs for the striatum, cortex

and cerebellum. The volumetric ROIs were then applied to the full dynamic data set to obtain the regional tissue time-radioactivity data.

2.4. Monkey microPET imaging

Studies were done in three young mature rhesus monkeys (6.7 - 7.5 kg). Animals were anesthetized (isoflurane) and intubated, a venous catheter inserted into one hindlimb and the animal positioned on the bed of the Concorde MicroPET P4 gantry. Isoflurane anesthesia was continued throughout the study. After completion of the transmission scan, animals were injected with (-)-[^{18}F]FEOBV (3.3 – 3.88 mCi, < 0.25 micrograms; in 1–3 ml isotonic saline) as a bolus over 1-2 min. Emission data was collected for 90 or120 minutes (frames from progressing from 1 to 10 min). Emission data were corrected for attenuation and scatter and reconstructed using the 3D maximum a priori method (3D MAP algorithm). Using a summed image of the last three frames (either 60-90 or 90-120 min data), ROIs were drawn manually on multiple planes to obtain volumetric ROIs for the striatum, thalamus, cortex and cerebellum. The volumetric ROIs were then applied to the full dynamic data set to obtain the regional tissue time-radioactivity data.

3. Results

3.2. Regional mouse brain biodistribution and blocking studies

At three hours after bolus iv injection of (-)-[^{18}F]FEOBV, there was a clear heterogeneous distribution of radioactivity in the mouse brain (striatum > cortex > hippocampus > thalamus > cerebellum) consistent with the distribution of cholinergic synapses and VAChT. Administration of doses of cold (-)-FEOBV reduced the retention of radioactivity in regions of high VAChT concentrations (striatum and cortex) at the 5 and 10 microgram/kg doses (Table 1).

3.2. Rat microPET imaging

Following bolus iv injection, (-)-[^{18}F]FEOBV rapidly entered the rat brain with a peak uptake at 3-4 minutes in striatum, cortex and cerebellum (Fig. 1). Selective retention of radioactivity was evident in the striatum and cortex, both of which were significantly higher than cerebellum after 20 minutes and which reached tissue concentration ratios of striatum/cerebellum = 2.3-2.4 and cortex/cerebellum = 1.3-1.4 at the end of the scan period.

3.3. Monkey microPET imaging

Representative tissue time-radioactivity curves for striatum, thalamus, cortex and cerebellum for the full 120 min following bolus injection of (-)-[^{18}F]FEOBV are shown in Fig. 2. Similar to the rat studies, the radioligand is rapidly taken up into brain tissue: as the radiotracer was injected as a slow bolus, a sharp peak for the maximum uptake point was not observed. In the cortex and cerebellum, significant washout of radioactivity occurred following the peak uptake. Radioactivity concentration in the thalamus continued to increase and nearly reached a plateau, but the striatal concentration continued to increase slowly throughout the entire 120 minute imaging session. Maximum tissue concentrations reached at the end of the scan were striatum/cerebellum = 3.96, thalamus/cerebellum = 3.47, and cortex/cerebellum = 1.79, providing unequivocal regionally specific retention in the monkey brain (Fig. 3). In the other two monkey studies, similar initial uptake and shapes of the regional tissue time-radioactivity curves were obtained although tissue concentration ratios varied between animals, and for the group of three animals a range of values for striatum/cerebellum (5.66, 2.54 and 3.96, average 4.05 +/- 1.5), thalamus/cerebellum (3.62,1.81 and 3.47, average 2.96 +/- 1.0) and cortex/cerebellum (1.42,1.49 and 1.79, average 1.53 +/- 0.2) ratios were obtained.

4. Discussion

The synthesis of (-)-[^{18}F]FEOBV, in vitro characterization as a high affinity radioligand for the vesicular acetylcholine transporter (VAChT), and in vivo and ex vivo rodent studies had been reported from our laboratories more than a decade ago [12,13]. From those studies, and others completed but not reported, we had concluded that (-)-[^{18}F]FEOBV was a suitable candidate for further development into an in vivo PET imaging agent for the VAChT in the human brain, with potential applications in the study of cholinergic terminal losses in neurodegenerative disease. The recent publication by Giboureau et al [10] questioned that decision, as those authors made a final conclusion that fluoroalkoxybenzovesamicols such as (-)-[^{18}F]FEOBV and the fluoropropyl analog [^{18}F]FEOPV had no future as in vivo imaging agents. In this paper we have examined (-)-[^{18}F]FEOBV in three different species (mouse, rat and rhesus monkey) and conclude, much as we had done years before, that this radioligand is indeed a suitable in vivo radioligand for imaging of the VAChT in the mammalian brain.

The ex vivo dissection studies of rodent brains form an excellent screening tool for evaluating regional uptake and pharmacological specificity of potential in vivo radioligands. Earlier studies with (-)-[^{18}F]FEOBV had demonstrated a heterogeneous distribution and retention consistent with the expected distribution of cholinergic terminals [13], and similar to that seen before using other radiolabeled VAChT radioligands [2,3]. Our previous in vivo studies with both of the two stereoisomers of FEOBV, as well as similar in vivo studies with the (+)- and (-)-isomers of a carbon-11 labeled analogue N-methylaminobenzovesamicol ([^{11}C]MABV), had clearly demonstrated that affinity for the vesicular transporter site resided only in the (-)-isomers (8), and care was taken to utilize only pure (-)-isomers in these current in vivo PET studies. The previous study had also demonstrated that drugs with high-affinity binding to sigma receptors did not alter in vivo uptake or distribution of (-)-[^{18}F]FEOBV, but had not reported studies aimed at the pharmacological blocking of the specific VAChT binding sites directly. In this study we have examined the effect of co-administration of unlabeled (-)-FEOBV for potential blocking of in vivo radioligand accumulation. At the 5 and 10 microgram/kg doses, a portion of the specific binding in the striatum and cortex could be blocked; higher doses could not be successfully used due to significant peripheral pharmacological effects resulting in deaths of animals. We had previously observed that attempts to block brain uptake and retention of [^{11}C]MABV using vesamicol had produced only a partial block [8]; consistently, we have observed that it is very difficult to administer enough cold mass of a VAChT inhibitor to occupy all brain sites without causing peripheral toxicity.

The microPET imaging of the rat brain uptake and localization of (-)-[^{18}F]FEOBV was successful in clear identification of good radiotracer retention in the striatum, intermediate in cortex, and low in cerebellum. Our in vivo PET imaging results in rats are similar to those recently reported by others [14] and are consistent with our prior ex vivo autoradiography studies of (-)-[^{18}F]FEOBV binding to the transporter in the rat brain [13]. Blocking studies were not attempted in our rat microPET imaging studies as the peripheral pharmacological effects of a VAChT inhibitor, manifested as severe breathing difficulties, would likely only be exacerbated by the general anesthesia (isoflurane) needed for the imaging procedure.

Monkey imaging studies are reported here for the first time (although we had actually successfully imaged (-)-[^{18}F]FEOBV in the monkey brain in 1992: Kilbourn and Mulholland, unpublished results), demonstrating a heterogenous regional retention of radioactivity in the monkey brain (Fig. 3). The regional distribution of striatum > thalamus > cortex > cerebellum is consistent with what might be expected based on rodent data, but unfortunately there are no comprehensive data for regional distributions of the VAChT in the primate brain. The tissue time-radioactivity curves (Fig. 2) showed retention of the radioligand in the striatum and thalamus, with significant washout from the cerebellum and intermediate retention in the

cortex. At the end of the scan period of 90 minutes the striatum to cerebellum ratio has reached a value of almost four to one, significantly better than that obtained with the recently reported o-[^{11}C]methylvesamicol [11]. The radioligand appears not to undergo significant defluorination to produce [^{18}F]fluoride. No attempts have been made to perform blocking studies using a cold mass of a vesamicol derivative, as it was deemed not ethical to chance toxic peripheral effects in this species. The monkey imaging results reported here for (-)-[^{18}F]FEOBV are decidedly different than reported by Giboureau et al [10] for the propyl derivative [^{18}F]FPOBV, where an essentially homogeneous brain distribution was observed, along with significant evidence of defluorination. It should be noted that Giboureau et al [10] did not report any PET imaging studies with (-)-[^{18}F]FEOBV but simply generalized the [^{18}F]FEOPV results to both radiotracers.

We thus have verified our prior observations with (-)-[^{18}F]FEOBV in the rodent brain and further demonstrated its imaging potential in the non-human primate brain. The previous conclusions of Giboureau et al that (-)-[^{18}F]FEOBV appears "…unsuitable for in vivo imaging of the VAChT using PET…" (10) are inconsistent with our data, although we note that their conclusion was based solely on a single ex vivo dissection study of the radioligand in the rat brain and no dynamic PET imaging in rat or monkey was done. The reasons for this difference, which could be due to stereoisomeric purities, species or strain differences, anesthesia, or simply experimental design and execution, remain unresolved.

Based on our now extensive studies in three species (mouse, rat and monkey), using the techniques of ex vivo autoradiography, ex vivo dissection, and in vivo PET imaging, the compound (2*R*,3*R*)-5-[^{18}F]fluoroethoxybenzovesamicol ((-)-[^{18}F]FEOBV) remains a viable and exciting in vivo radioligand for VAChT imaging in the mammalian brain.

Acknowledgement

This work was supported by grants from the National Institutes of Health (MH66506) and the Office of Science, US Department of Energy (DE-FG02-87ER60561).

References

1. Parsons SM, Prior C, Marshall IG. Acetylcholine transport, storage and release. Int Rev Neurobiol 1993;35:279–390. [PubMed: 8463062]
2. Frey, KA.; Wieland, DM.; Kilbourn, MR. Imaging of monoaminergic and cholinergic vesicular transporters in the brain. In: Goldstein, D.; Eisenhofer, G.; McCarty, R., editors. Catecholamines: Bridging Basic Science with Clinical Medicine. Academic Press; San Diego: 1997. p. 269-272.
3. Efange SM. In vivo imaging of the vesicular acetylcholine transporter and the vesicular monoamine transporter. Faseb J 2000;14:2401–13. [PubMed: 11099458]
4. Kuhl DE, Minoshima S, Fessler JA, Frey KA, Foster NL, Ficaro EP, Wieland DM, Koeppe RA. In vivo mapping of cholinergic terminals in normal aging, Alzheimer's disease, and Parkinson's disease. Ann Neurol 1996;40:399–410. [PubMed: 8797529]
5. Albin RL, Cross D, Cornblath WT, Wald JA, Wernette K, Frey KA, Minoshima S. Diminished striatal [^{123}I]iodobenzovesamicol binding in idiopathic cervical dystonia. Ann Neurol 2003;53:528–32. [PubMed: 12666122]
6. Gilman S, Chervin RD, Koeppe RA, Consens FB, Little R, An H, Junck L, Heumann M. Obstructive sleep apnea is related to a thalamic cholinergic deficit in MSA. Neurology 2003;61:35–9. [PubMed: 12847153]
7. Mazere J, Prunier C, Barret O, Guyot M, Hommet C, Guilloteau D, Dartigues JF, Auriacombe S, Fabrigoule C, Allard M. In vivo SPECT imaging of vesicular acetylcholine transporter using [(^{123}I)]-IBVM in early Alzheimer's disease. Neuroimage 2008;40:280–8. [PubMed: 18191587]

8. Kilbourn MR, Jung Y-W, Haka MS, Gildersleeve DL, Kuhl DE, Wieland DM. Mouse brain distribution of a carbon-11 labeled vesamicol derivative: presynaptic marker of cholinergic neurons. Life Sciences 1990;47:1955–63. [PubMed: 2266779]

9. Widén L, Eriksson L, Ingvar M, Parsons SM, Rogers GA, Stone-Elander S. Positron emission tomographic studies of central cholinergic nerve terminals. Neurosci Lett 1992;136:1–4. [PubMed: 1321961]

10. Giboureau N, Emond P, Fulton RR, Henderson DJ, Chalon S, Garreau L, Roselt P, Eberl S, Mavel S, Bodard S, Fulham MJ, Guilloteau D, Kassiou M. Ex vivo and in vivo evaluation of (2R,3R)-5-[^{18}F]-fluoroethoxy- and fluoropropoxy-benzovesamicol, as PET radioligands for the vesicular acetylcholine transporter. Synapse 2007;61:962–70. [PubMed: 17787004]

11. Shiba K, Nishiyama S, Tsukada H, Ishiwata K, Kawamura K, Ogawa K, Mori H. The potential of (-)-o-[^{11}C]methylvesamicol for diagnosing cholinergic deficit dementia. Synapse 2009;63:167–171. [PubMed: 19021207]

12. Mulholland GK, Jung Y-W, Wieland DM, Kilbourn MR, Kuhl DE. Synthesis of [^{18}F]fluoroethoxy-benzovesamicol, a radiotracer for cholinergic neurons. J Labelled Compds Radiopharm 1993;33:583–91.

13. Mulholland GK, Wieland DM, Kilbourn MR, Frey KA, Sherman PS, Carey JE, Kuhl DE. [^{18}F] Fluoroethoxy-benzovesamicol, a PET radiotracer for the vesicular acetylcholine transporter and cholinergic synapses. Synapse 1998;30:263–74. [PubMed: 9776130]

14. Rosa-Neto P, Alliaga A, Mxengeza S, Massarweh G, Landry E, Bedard M-A, Soucy J-P. Imaging vesicular acetylcholine transporter in rodents using [^{18}F]fluoroethoxy-benzovesamical and microPET. J Cer Blood Flow Metab 2007;27(Suppl 1):PP03–07M.

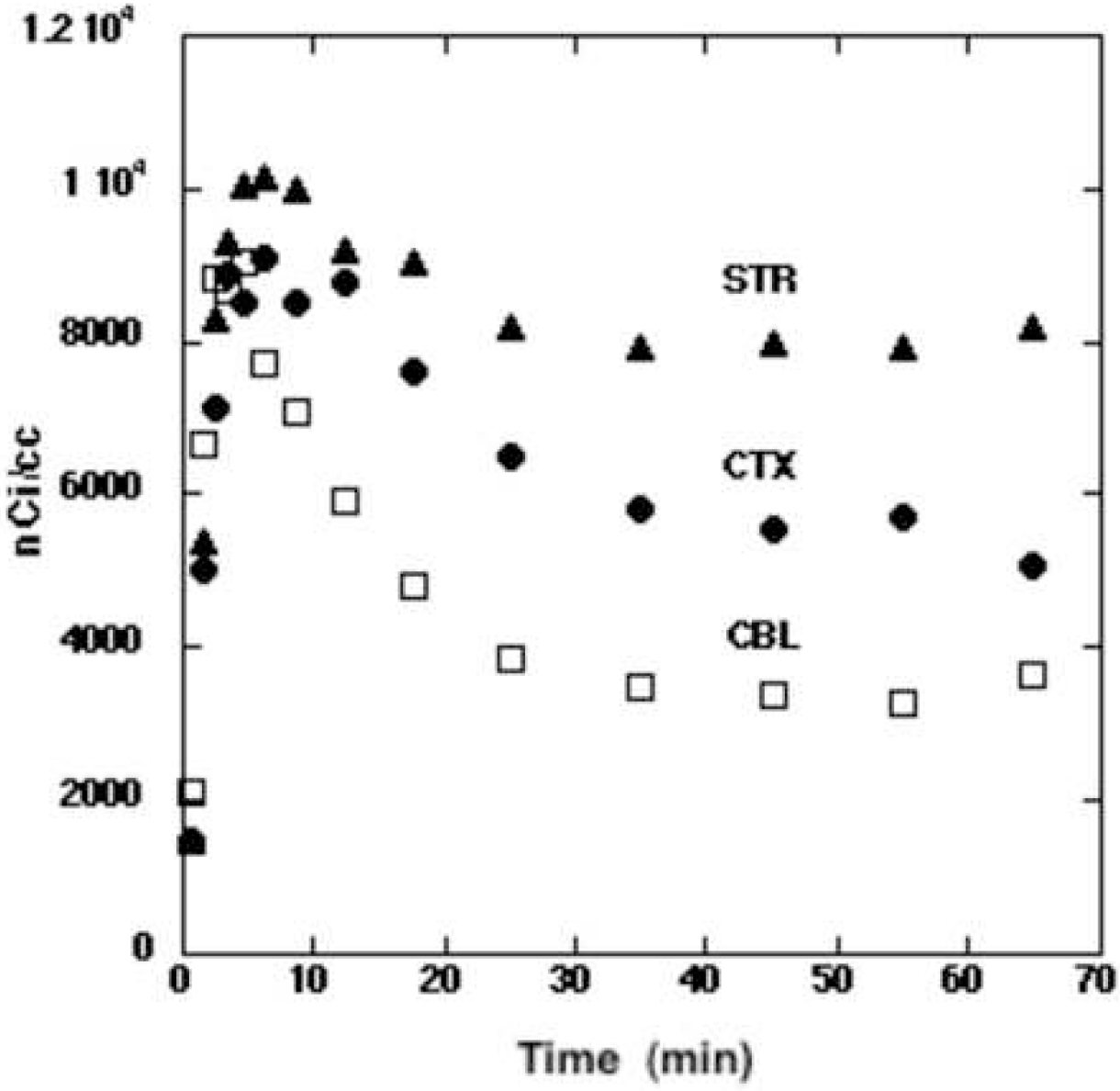

Fig. 1.
Representative tissue time-radioactivity concentration curves for microPET imaging of (-)-[18F]FEOBV in rat brain following bolus iv injection. STR = striatum, CTX = cortex, CBL = cerebellum.

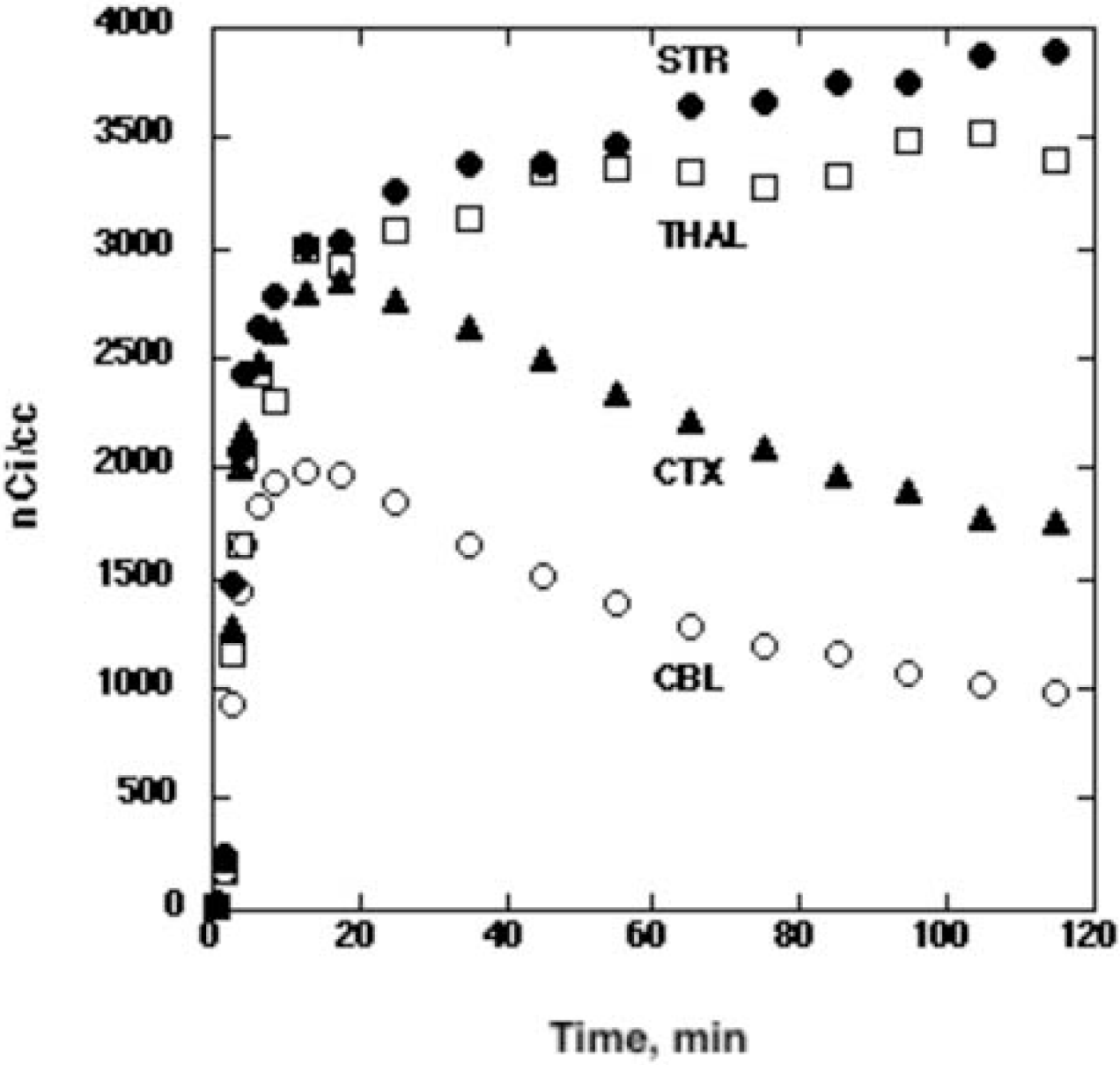

Fig. 2.

Representative tissue time-radioactivity concentration curves for microPET imaging of (-)-[18F]FEOBV in rhesus monkey brain following bolus iv injection. STR = striatum, CTX = cortex, THAL = thalamus, CBL = cerebellum.

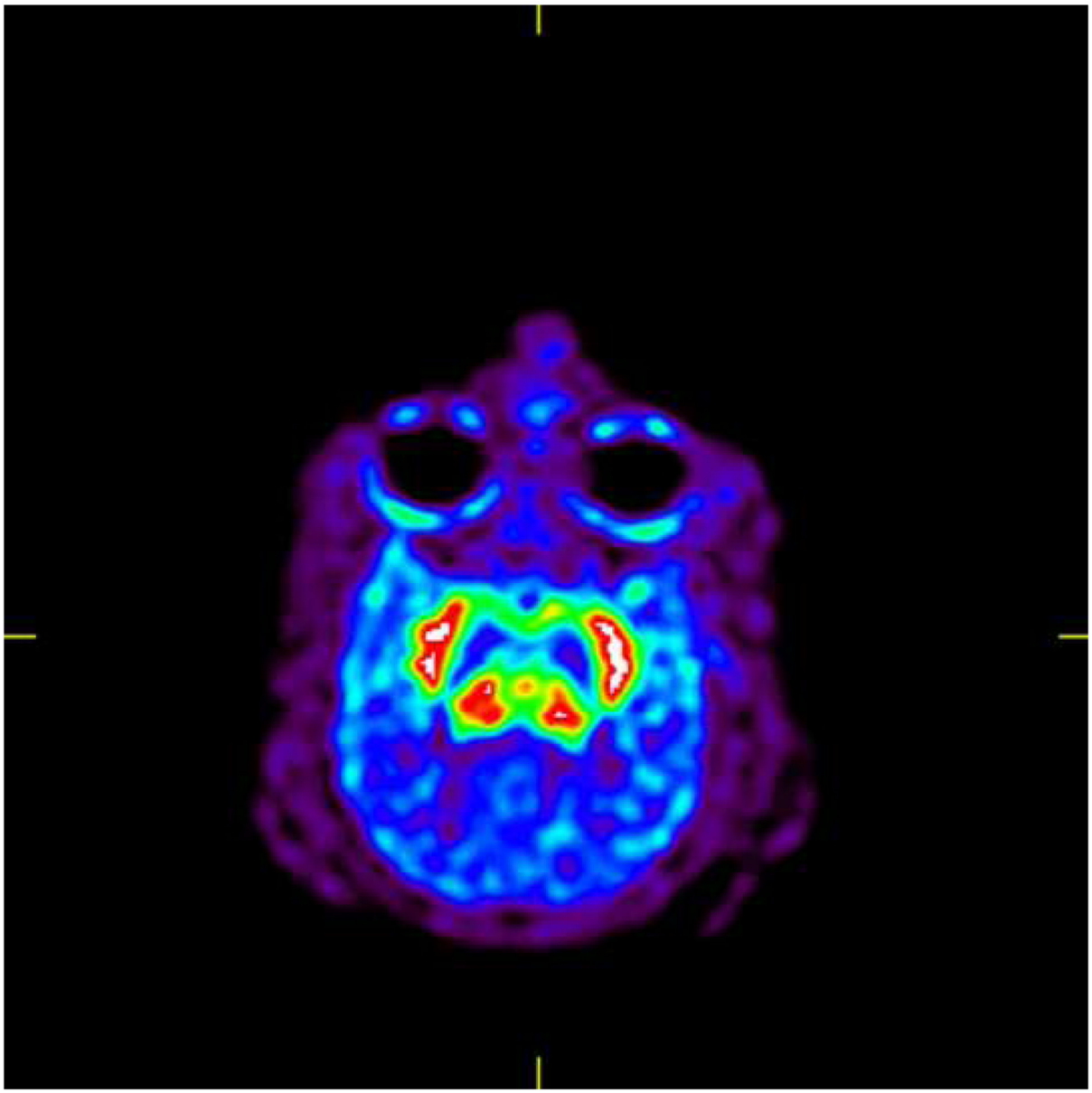

Fig 3.
PET image of (-)-[18F]FEOBV uptake into rhesus monkey brain (transaxial image at 90-120 min).

Table 1

Dose-dependent blocking of [18F]FEOBV in mouse brain striatum and cortex using unlabeled FEOBV co-administration. STR/CBL and CTX/CBL are striatum- and cortex-to-cerebellum ratios determined by dissection at three hours after radiotracer injection.

FEOBV dose	STR/CBL	CTX/CBL
0 (control)	4.95 +/- 0.93	2.76 +/- 0.89
2 μg/kg	4.53 +/- 0.49	2.70 +/- 0.28
5 μg/kg	4.35 +/- 0.59	2.72 +/- 0.31
10 μg/kg	3.58 +/- 0.14	2.14 +/- 0.15